


Exploring Mechanisms Underlying Unexplained Air-Bone Gaps Post-Myringoplasty: Temporal Bone Model and Finite Element Analysis

Ear, Nose & Throat Journal
2022, Vol. 0(0) 1–9
© The Author(s) 2022
Article reuse guidelines:
sagepub.com/journals-permissions
DOI: 10.1177/01455613221120371
journals.sagepub.com/home/ear
SAGE

Jie Wang, MD^{1,2}, Xingmei Wei, MD¹ , Ying Zhang, MD³, Takuji Koike, PhD⁴, Sinyoung Lee, PhD⁴, Yongxin Li, PhD¹, and Fei Zhao, MD⁵

Abstract

Purpose: Air-bone gap (ABG) is an essential indicator of middle ear transfer function after myringoplasty. However, there is still uncertainty about the mechanisms behind unexplained ABGs in patients post-myringoplasty. The present study investigated these mechanisms using cadaveric temporal bone (TB) measurement and finite element (FE) modeling. **Methods:** Three conditions of tympanic membrane (TM) perforation were modeled with a perforated area of 6%, 24%, and 50% of the total TM area to simulate a small, medium, or large TM perforation of TB model. A piece of paper was used to patch the TM perforation to simulate the situation post-myringoplasty. In the FE model for post-operation, the material properties at the perforation area were changed. Measurement of TM vibration at the umbo was undertaken with a laser Doppler vibrometer (LDV). **Results:** As the perforated area increased vibration of the TM at the umbo decreased in both the TB and FE models. But the reduction of TM vibration is more minor in the FE model than in the TB model. After the perforation was repaired, the displacement of TM at the umbo could not be recovered totally in the TB and FE models. In the FE model, the displacement of TM at the umbo decreased markedly when the cone shape of TM flattened, and the reduction was almost the same as that in the TB model in the condition of large perforation. **Conclusion:** The material properties and the anatomical shape of the repaired TM could influence the TM's modal motion and wave motion. Except for appearance and shape current clinical instruments are unable to resolve factors that affect TM motion. Consequently the ABG seen post-myringoplasty remains unexplained.

Keywords

myringoplasty, air-bone conduction gap, tympanic membrane perforation, laser Doppler vibrometer, finite element model

Introduction

Tympanic membrane (TM) perforation is commonly caused by a middle ear infection, trauma, or rapid change in pressure. Tympanic membrane perforation typically leads to conductive hearing loss (CHL) and several aural symptoms such as earache and recurrent drainage.¹ In general, patients with a TM perforation show mild to moderate hearing loss in air conduction (AC) but show a normal hearing threshold for bone conduction (BC). The AC and BC hearing threshold gap Air-bone gap (ABG) is typically greater than 10 dB, which is a critical audiological criterion used to distinguish between conductive and sensorineural hearing loss.²

¹Department of Otolaryngology-Head and Neck Surgery, Beijing Tongren Hospital, Key Laboratory of Otolaryngology-Head and Neck Surgery, Ministry of Education, Capital Medical University, Beijing, China

²Beijing Engineering Research Center of Audiology Technology, Beijing, China

³Department of Otolaryngology-Head and Neck Surgery, 263 Clinical Department of the Army General Hospital, Beijing, China

⁴Department of Mechanical and Intelligent Systems Engineering, Graduate School of Information and Engineering, The University of Electro-Communications, Tokyo, Japan

⁵Centre for Speech and Language Therapy and Hearing Science, Cardiff School of Sport and Health Sciences, Cardiff, UK

Received: May 18, 2022; revised: July 14, 2022; accepted: August 1, 2022

Corresponding Author:

Zhao Fei, Centre for Speech and Language Therapy and Hearing Science, Cardiff School of Sport and Health Sciences, Cardiff, UK.
Email: fzhao@cardiffmet.ac.uk



Creative Commons Non Commercial CC BY-NC: This article is distributed under the terms of the Creative Commons Attribution-NonCommercial 4.0 License (<https://creativecommons.org/licenses/by-nc/4.0/>) which permits non-commercial use, reproduction and distribution of the work without further permission provided the original work is attributed as specified on the SAGE and Open Access pages (<https://us.sagepub.com/en-us/nam/open-access-at-sage>).

Myringoplasty is a standard surgical procedure for repairing the TM, aiming to close the TM perforation and thus protect the middle ear mucosa from infection and, more importantly, restore hearing.³ Evidence shows that approximately 80–90% of cases have a hearing improvement of 9.6–15.0 dB in AC hearing thresholds.^{4–6} Although many patients have a minimal ABG post-myringoplasty reported in numerous studies, a proportion of patients unexpectedly show a large post-operative ABG. For example, Shrestha and Sinha⁷ showed that post-operative ABG was less than 10 dB in only 22% of cases, with many patients (62%) showing an ABG greater than 10 dB. Pfammatter and Linder⁵ revealed a zero ABG in only 20% of 106 patients, and a mean residual ABG of 8 dB in 80% of cases. It is noteworthy that there is a large post-operative ABG in some cases even after the perforated TM is closed.

Several factors are proposed to affect post-operative ABGs, such as the thickness of the reconstructed TM, malfunction of the middle ear cavity mucosa and Eustachian tube dysfunction.⁸ However, uncertainty remains as to the mechanisms underlying the unexpected ABGs in patients' post-myringoplasty, even when the reconstructed TM restores the normal anatomic characteristics.

The modal motion of the TM transfers sound energy to the manubrium of the malleus. Factors that decrease movement of the TM could reduce the transfer function of the TM.⁹ Therefore, after myringoplasty, the material properties of the reconstructed TM, that is, stiffness, and thickness, could influence vibration of the TM.^{10,11} Several studies have shown that the reconstructed TM might have different sound transmission properties due to radial collagen damage by the TM perforation that cannot be restored by the myringoplasty.^{12,13}

A finite element (FE) model of the human middle ear allows a theoretical prediction of TM perforation effect on middle ear transfer function. Previous studies have shown that anatomic and acoustic properties of the reconstructed TM influence the TM's vibration, and consequently, post-operative ABGs.^{10,12,14,15} For example, Koike et al¹¹ used a FE model of the TM to show that transfer function varied with the TM's anatomic shape and physical properties, that is, depth of conical shape and stiffness of the TM. Mostafa et al¹⁶ report a temporal bone (TB) study using cartilage and perichondrium as graft materials to simulate myringoplasty and measured vibration at the umbo and stapes. However, neither cartilage, perichondrium, or measurement of stapes vibration is available in ENT outpatient clinics. Voss et al¹⁷ and Roosli et al¹⁸ measured middle ear transfer function using a TB model of TM perforation with stapes motion, but this experimental approach is not suitable for the clinical use.

The paper patch test^{19,20} uses a piece of paper to cover a TM perforation and simulate the intact TM condition. This is helpful to evaluate the post-operative hearing level of a successful TM perforation repair of an outpatient with a TM perforation less than 4–5 mm.^{20,21} Therefore, use of a paper patch using a cadaveric TB model would be helpful to the ear surgeon to analyze ABG post-myringoplasty more effectively.

The present study further explores the bio-mechanic factors underlying unexpected post-operative ABGs by comparing the outcomes of FE model analysis and TB experiments. This study's novelty is to provide a comprehensive understanding of the relationships between repaired TM vibration and ABGs after myringoplasty.

Materials and Methods

Human Cadaveric TB Model and Measurement

Four fresh cadaveric human TB without a history of ear disease were prepared. Normality of the TM was confirmed endoscopically. Normal middle ear structure, that is, middle ear cavity and the ossicular chain was also checked. The cartilaginous part of the external auditory canal was then removed to better expose the TM. A laser Doppler vibrometer (LDV) (Polytec. CLV-2534) was used to measure vibration of the TM at the umbo. A 90 dB SPL pure tone at frequencies of 500, 1000, 2000, and 4000 Hz (generated by an Agilent 33210A waveform generator) was applied to the TM. At the same time, a monitoring microphone (Etymotic Research, ER-7C Series B) was located approximately 2 mm lateral to the umbo.

After the transfer function of the normal TM was measured, 3 different sized perforations, small, medium, and large were simulated:

- (1) The small perforation was achieved by cutting the anteroinferior part of the TM with an excision knife to make a perforation of approximately 6% of the total TM area (Figure 1A). After perforation the vibrations of the umbo and short process of the TM were tested. The perforation was then covered with a 0.1 mm thick paper patch that extended 1–2 mm beyond the edge of the perforation (Figure 1B).
- (2) The medium-sized perforation had the perforation enlarged to approximately 23% of the total TM area (Figure 1C). Following testing, the perforation was covered with a paper patch for further measurements (Figure 1D).
- (3) The large perforation covered approximately 50% of the total TM area (Figure 1E). Measurements and paper patching were carried out as with the small and medium models (Figure 1F).

Finite Element Modeling

The FE model of the human middle ear used in the present study was constructed following the initial FE model developed by Koike et al.¹¹ The model comprised the TM, ossicles and the vestibular part of the cochlea. Each parameter was determined from the reported values.¹¹ The unknown parameters were determined by confirming calculation results to the values of the measurements.⁴ The more detailed characteristics of this FE model in the published model by Koike et al.¹¹

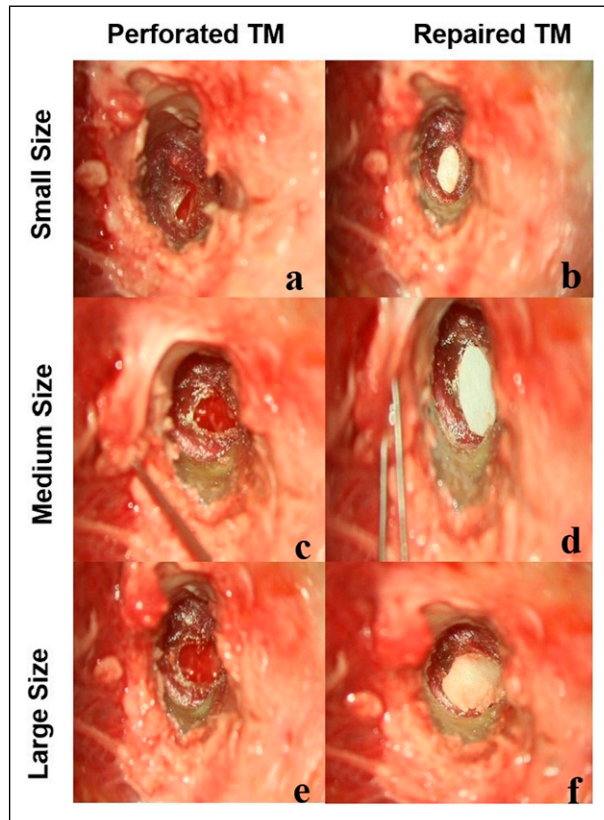


Figure 1. Human cadaveric temporal bone models of TM perforation in the left column marked **a**, **c**, and **e**, and the paper patched models shown in the right column labeled **b**, **d**, and **f**.

In this study, we simulated the condition of repaired TM by modifying stiffness and density in the repaired perforated area. Three different sized TM perforations in cone shape and flat condition were simulated to represent 5.61–5.87% (Perforation 1), 22.8–23.1% (Perforation 2), and 49.4–49.9% (Perforation 3) of total TM area. [Figure 2](#) shows front- and side-views of the FE model with the cone-shaped TM and flat-shaped TM.

The Young's modulus of the TM pars tensa and pars flaccida were 33.4 MPa and 11.1 MPa, respectively. The density of the TM is 1200 kg/m³. The density and Young's modulus of the repaired TM were changed as shown in [Table 1](#). In this study, consideration was given to the degree of fibrosis or scarring of the repaired TM with density and Young's modulus all increasing post-myringoplasty.²² As indicated in [Table 1](#), the density of the repaired TM was increased to 10 and 100 times that of the normal TM. Collagen fiber, a stiff biological fiber, is the main histological component of scar. Its Young's modulus is generally in a scale of a few GPa,²³ which is greater than that used in normal TM condition (ie, around 5–60 MPa).²⁴ As a result, we increased the Young's modulus of temporal fascia to 1000-fold and 10000-fold to simulate the condition of scarring. It should be noted that the shape of the repaired TM (coned and flattened) was also simulated in this study.

Harmonic response analyses were performed using CFD-ACE+ software (ESI Group) at frequencies between 500–

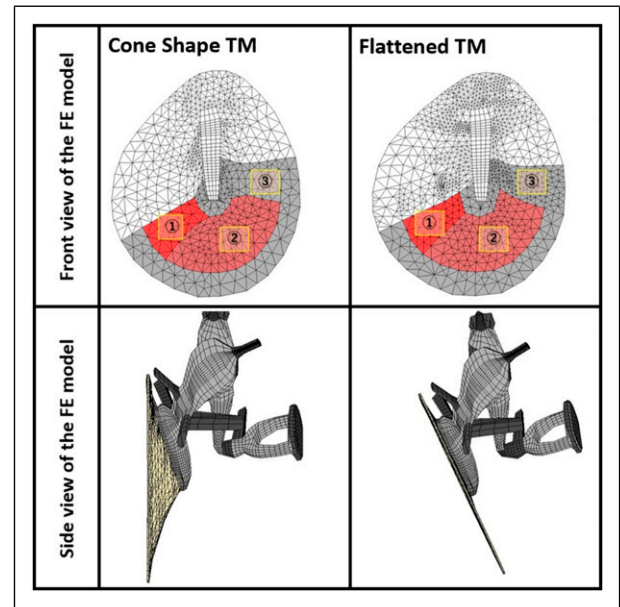


Figure 2. Finite element models of coned and flattened TM to simulate 3 perforation conditions. Left-side images show the cone-shaped TM and its side view in the FE model, and the right-side images show the flattened TM and its side view. The small perforation is marked as ① (hole 1), the medium perforation marked as ①+② (hole 2), and the large perforation marked as ①+②+③ (hole 3). The percentage of the perforated area of the TM is about 6%, 23%, and 50%, respectively.

8000 Hz when a pure tone of 90 dB SPL was applied at the TM. The detailed FE model conditions calculated the transfer functions under the different situations.

Data Analysis

The Umbo Velocity of Transfer Function (UVTF) was calculated by normalizing the velocity of the TM vibration at the umbo by the sound pressure level monitored at approximately 2 mm lateral to the TM. To confirm that the middle ear structures were functioning normally, we compared the cadaveric TB TM vibration with that measured on live humans. Measurement of displacement at the umbo was measured 5 times for each cadaveric TB model. The average value of all the measurements was compared with that of the FE model calculation. The TB and FE models' values were referenced with each normative data when calculating the displacement change on the dB scale.

Results

Temporal Bone Measurement

[Figure 3](#) shows that TM displacement at the umbo in the cadaveric TB was almost the same as that of live humans.²⁵ TM displacement at the umbo before and after a paper patch is shown in [Figures 4A and 4B](#) (referenced to the normal displacement of TM, in dB). The results show that as perforation area increased then displacement decreased across frequencies

Table 1. Properties of Tympanic Membrane Used in the Post-Myringoplasty FE Models.

		Young's Modulus [MPa] Temporal Fascia: 5.64 MPa (Trindade et al, 2012)	
		×1000	×10000
Density [kg/m³]	×10	Condition A1: Cone shape	Condition C1: Cone shape
Tympanic membrane		Condition A2: Flat shape	Condition C2: Flat shape
Normal value: 1200 kg/m ³ (Koike et al., 2002)	×100	Condition B1: Cone shape	
		Condition B2: Flat shape	

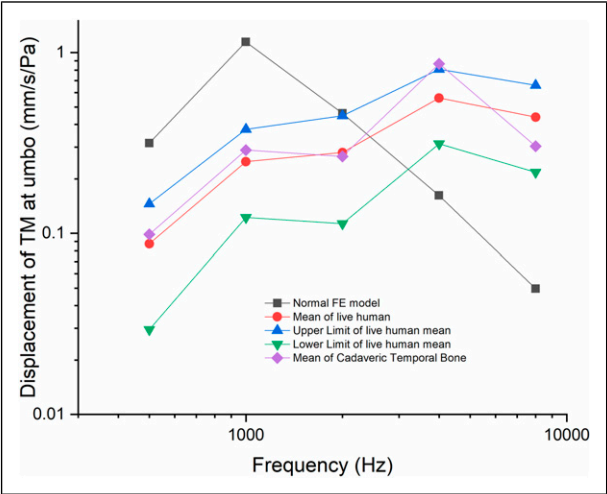


Figure 3. The calibration of the TB model and the FE model with the normative data from live humans.

500–8000 Hz. Following paper patching, In the case of a small hole, the displacement of TM was decreased in comparison to the post paper patched situation. However, the TM vibrations in the medium and large perforations were restored more markedly than in the case of the small perforation. Another characteristic was that there was relatively little change in TM vibration at 8000 Hz before and after patching and particularly so for the medium and large perforations. In addition, in the case of the large perforation, TM displacement decreased relatively markedly at 4000 Hz this reduced after patching.

Finite Element Modeling

The published data¹¹ verifies our FE model. In this study, three conditions of post-myringoplasty were simulated, and the vibration of TM was calculated with cone and flat shapes. Our results show that, as the TM perforation area increased, vibrations of the TM at the umbo reduced across frequencies 500 to 8000 Hz (Figures 5A–5F). The decrease was significant when the repaired TM was flattened. In Figures 6A–6C, we further compared the change of TM vibration with normative data of the FE model in dB.

Figures 5A and 5B show that the small perforation had little effect on vibration of the TM. After the hole was

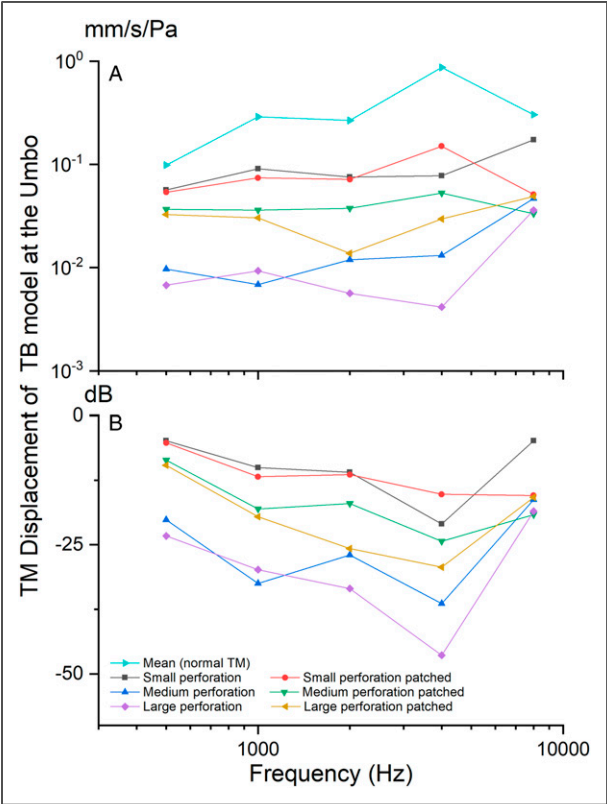


Figure 4. Tympanic membrane displacement at umbo in 3 perforation conditions using the TB model. (a) TM displacement (mm/s/Pa) at umbo in 3 perforation conditions using the TB model, (b) TM displacement (dB) at umbo after TM perforation repair using paper patching.

patched using paper and the TM flattened displacement of the TM decreased across all frequencies 500–8000 Hz (Figure 5A). In Figure 5B, with TM kept coned, vibrations of the TM decreased slightly and mainly at frequencies below 2000 Hz.

When perforation area was increased from 6% to 23% (medium perforation, Figures 5C and 5D), TM displacement at the umbo decreased across frequencies 500–8000 Hz, remarkably so when the density and stiffness of the repaired TM was increased 100 times and 1000 times. The effect was similar in the case of a large perforation (ie, about 50% of the total TM area (Figures 5E and 5F).

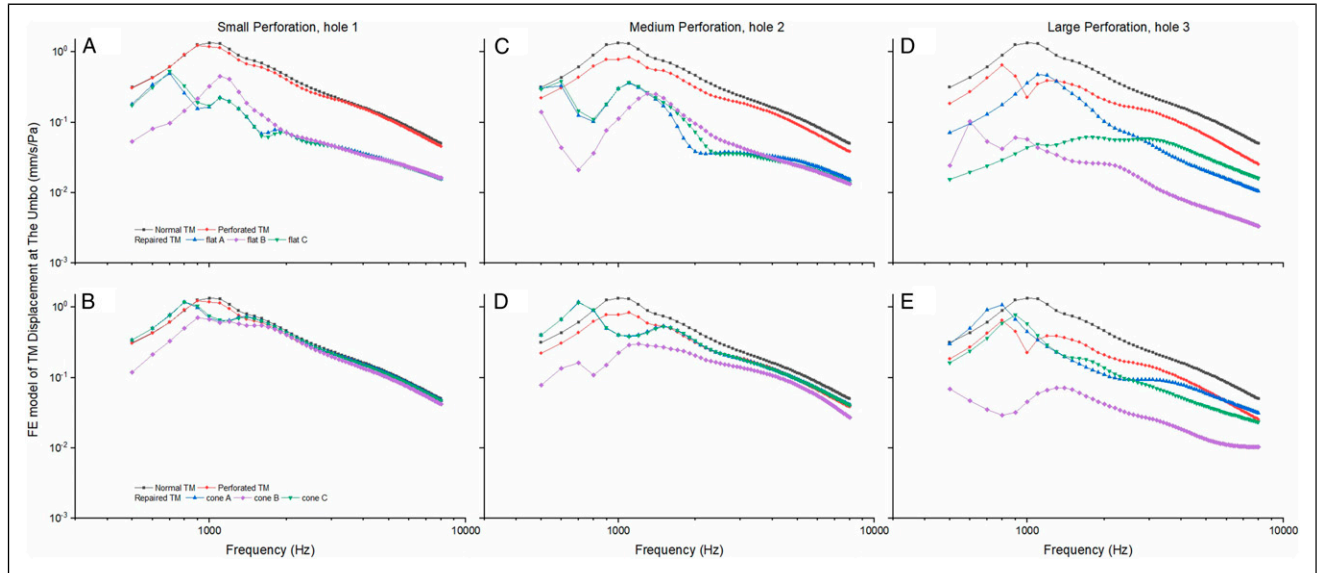


Figure 5. Calculation of TM vibration (mm/s/Pa) in 3 perforation conditions using the FE model. **5a, c and e:** calculation of the umbo displacement when simulating the flattened TM in small, medium, and large perforation conditions, respectively. **5b, d and f:** calculation of the umbo displacement when simulating the cone-shaped TM in small, medium and large perforation conditions, respectively.

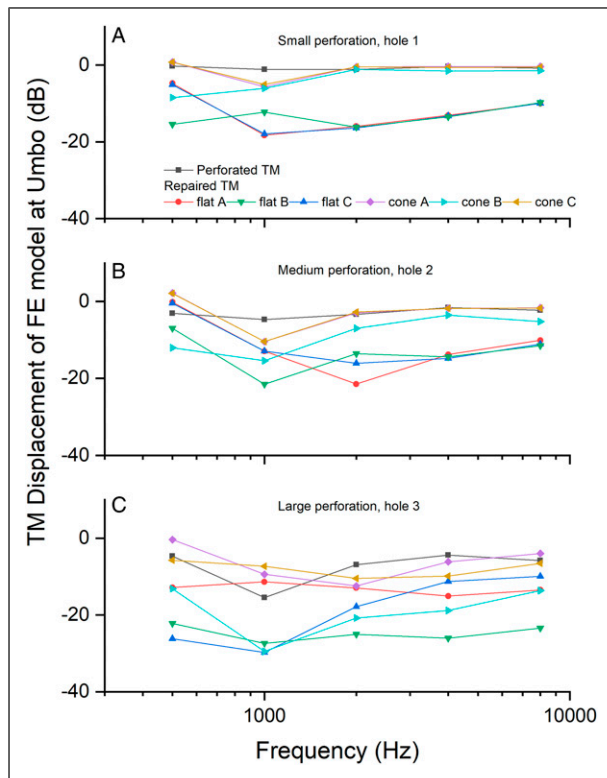


Figure 6. Calculation of The TM displacement (dB) at umbo using the FE models to simulate 3 perforation conditions (**a, b, and c**, respectively).

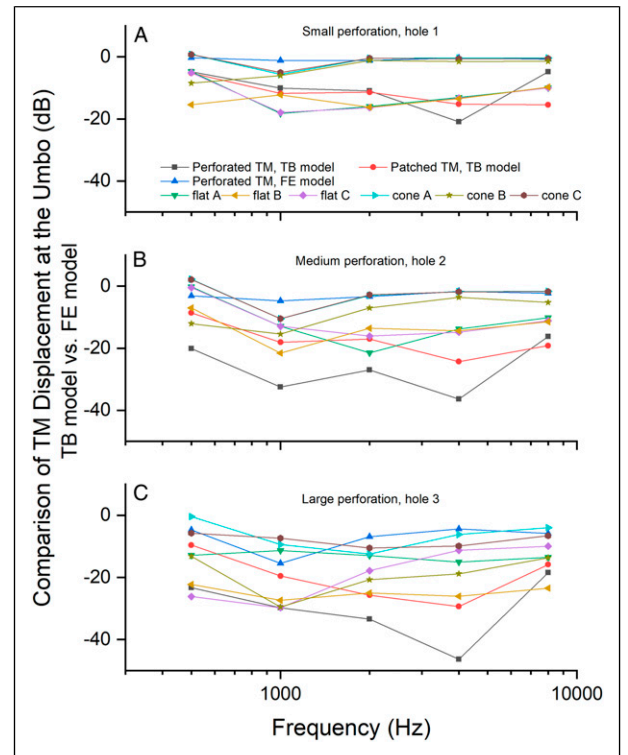


Figure 7. Comparison of the TM displacement at umbo between the TB and the FE models in 3 perforation conditions (**a, b, and c**, respectively).

Comparison of FE Modeling and Temporal Bone Measurement With Normal Data

Small perforation. A comparison of the normal FE model with the small perforation TB model (Figure 7A), shows a loss of TM displacement at the umbo of approximately 10 dB at 1000 and 2000 Hz, less than 5 dB at 500 and 8000 Hz, but a reduction of approximately 20 dB at 4000 Hz. After paper patching, the TM's vibration at the umbo was partially restored at 1000, 2000, and 4000 Hz, but reduced slightly at 8000 Hz.

In the FE model, vibration of the TM at the umbo changed slightly with the small perforation (hole 1), losing a few dB at 1000 Hz. When the repaired TM flattened, there was a greater loss at 1000 and 2000 Hz, approaching -20 dB, however this was better than the TB model at 4000 and 8000 Hz.

Medium perforation. As shown in Figure 7B, in the medium perforation case, vibration of the TM at the umbo reduced by approximately 30 dB at 1000 and 2000 Hz and less than 20 dB at 500 and 8000 Hz. It reduced to less than approximately 5 dB across the frequencies in the FE model.

After paper patching in the medium perforation TB model, there was a recovery to approximately 20 dB at 1000, 2000, and 8000 Hz, less than 10 dB at 500 Hz and less than 25 dB at 4000 Hz. In the FE models, almost all the vibrations of the TM at the umbo reduced after the density and stiffness changed. The effect was greater when the cone-shaped TM flattened, particularly in the case of flat B (thickness and stiffness of hole 2 changed to 100 times and 1000 times). It decreased to more than 20 dB at 1000 Hz, less than 15 dB at 2000, 4000, and 8000 Hz, and less than 10 dB at 500 Hz. Compared with the TB model, there was a greater loss in displacement in the FE model of flat B condition across 500–8000 Hz, except at 4000 Hz. At 4000 Hz the loss of TM vibration was only 3 dB higher than that of the FE model in the flat B condition.

Large perforation. Figure 7C shows the effect of the large perforation, with vibration of the cadaveric TM at the umbo decreased to approximately 30 dB at 1000 and 2000 Hz, 20 dB at 500 Hz and 8000 Hz, and 45 dB at 4000 Hz. In the FE model it is reduced by less than 10 dB at 500, 2000, 4000, and 8000 Hz, and decreased markedly to about 15 dB at 1000 Hz. In the TB model, after paper patching displacement was restored to more than 25 dB at 2000 and 4000 Hz, less than 20 dB at 1000 and 8000 Hz, and less than 10 dB at 500 Hz. In the FE model, the vibration of the TM at the umbo was also reduced, and worse where the cone-shaped TM changed to flattened. In addition, as shown in Figure 7C (FE model flat C), the umbo displacement reduced markedly when the density of the perforation area increased by 100 times, and the vibration decreased by 30 dB at 1000 Hz, greater than 25 dB at 2000 and 4000 Hz, and more than 20 dB at 500 and 8000 Hz.

Discussion

Air-Bone Gap Values and Size of Perforation

The results of this study show that TM vibration at the umbo decreased with increase in size of TM perforation in both TB and FE models. Previous experimental, theoretical and clinical studies^{17,26,27} have shown that ABG depends on the size of the TM perforation, rather than the location of the TM.²⁸⁻³⁰ We also found that the ABG could not be closed in the TB and FE models after the TM perforation was repaired. Our TB model showed a loss of TM displacement at the umbo after the small hole was patched with paper similar to the FE models. Even with the medium and large perforations, in neither the TB models nor the FE models was there a recovery of the TM vibration at umbo. Pfammatter et al⁵ also observed that only 20% of myringoplasty cases could reduce the ABG within 5 dB, and 80% of patients presented 8 dB ABG in all cases, which is similar to the findings in the TB models and FE models.

Air-Bone Gap Values and the Material Properties of Repaired TM

It is generally noted that the repaired TM appears thickened post-myringoplasty. Given that the clinical CT scanning resolution is .5–.625 mm, the thickness of the repaired TM should be more than .5 mm,³¹ which is thicker than in the TB model. Lee et al¹⁴ reported that the thickness of the repaired TM is one of the critical factors that influence TM vibration. However, we used A4 office printing paper to patch the TM perforation in the TB models. Its thickness is about 0.1 mm, its density is 310 kg/m³, and Young's modulus is .1 GPa.³² In this study, although the thickness of the paper patch was almost the same as that of the normal TM, the ABG was still present after the paper patch repaired the perforation in the TB model. This indicates that mechanical properties are important for post-myringoplasty ABG.

Previous studies have shown a stiffness increment caused by scar formation in the repaired area of TM post-myringoplasty.^{33,34} However, the stiffness of the perforated area of TM was 1000 and 10000 times than that of the normal TM in our FE model, which is similar to the mechanical properties of collagen fibers.³⁵ Our results showed that the displacement of TM at the umbo decreased in all sizes of TM perforations, and with the stiffness increased, the vibration of TM at the umbo decreased accordingly, particularly where the density increased 100 times (flat B). Therefore, Young's modulus of TM is a crucial mechanical property in terms of restoring the TM's normal vibration. This result is consistent with the findings reported by De Greef.³⁶ The authors investigated the effect of TM parameter values on the FE modeling, and their data also showed that Young's modulus of the TM is one of the most critical parameters in calculating middle ear transfer function.

The fiber arrangement of the TM is another crucial parameter for normal vibration of the TM. After the TM perforation

is repaired, scar formation is unavoidable, and the fiber arrangement of the scar is disorganized. In the normal structure of TM, the regular arrangement of circumferential and radial fiber keeps the TM functional.^{33,37} In this study, a fiber arrangement was absent in the TB and FE models. Clinically, the repaired TM also shows unarranged fibers in the repaired area.

The Influence of Repaired TM Shape on the TM Vibration Characteristics

In the FE models of this study, where the TM was flattened, displacement of TM at the umbo decreased markedly, in agreement with Koike et al.^{9,11,22} In the TB models, a piece of patched paper is different to that of the normal TM that could keep its cone shape. Consequently a shape change to flat also contributes to the loss of TM vibration in the TB model of this study.

Normal vibration of the TM is required to effectively couple sound energy to the manubrium of the malleus. Vibration quality decides whether the TM is functioning normally. The global material properties of the TM and its boundary conditions determine the TM displacement according to the modal motion feature the same as that of standing wave.⁹ Most of the published middle ear FE models are based on modal theory.^{9-11,14} In this study, the FE model calculation showed that the material properties of the TM have a marked influence on the displacement of the TM. With increases in density and stiffness, the vibration of the TM decreased accordingly. In the TB model, Young's modulus of the repairing materials was reduced, and the vibration of the TM was also reduced.

The wave motion theory of TM^{9,38,39} argues that the local mechanical properties of the TM influence the coupling of sound energy through the TM to the ossicles. This data^{38,39} shows a time delay between TM motion and stapes motion of approximately 20 μ s, with the delay time increasing with a larger TM area. Parent and Allen^{38,40} showed that the cone-shaped TM helps wave transformation from the tympanic ring to the umbo. Rosowski et al.⁹ further indicated that the local pathology of TM had a limited effect on the TM's modal motion. However it still had a marked influence on the waving motion of TM, significantly when the rim of the TM was disrupted. Eldaibes et al.¹⁶ also suggests that the disrupted annular has a significant influence on the vibration of the TM at low frequencies.

This wave motion theory can explain why the perforation FE models in this study have limited effects on the TM's vibration at the umbo. Still, the displacement of the TM of TB models decreased markedly after the TM was perforated. In the TB models of this study, the perforation reached the umbo and the rim of the TM, and the paper patch covered the annular of the TM, which could influence the waving motion except

for the modal movement. Thus, our results show a marked loss of TM displacement in the TB model.

The Discrepancy Between Clinical Data and Experimental Study

Theoretically, after the TM perforation is repaired, the vibration of the TM should be near normal. However, the TB and FE models in this study and in the published data⁵ all indicate that the transfer function of the middle ear could not be restored to normal. Namely, a CHL or an ABG is still present. Except for the distinguishing influence factors, such as marked abnormal TM geometry, inflammation of middle ear mucosa, and Eustachian tube dysfunction, a proportion of cases show an unexplained ABG using clinical data.^{5,25}

The paper-patch technique is effective for repairing small TM perforations.²¹ In this technique, a piece of paper is used as a scaffold and placed on the rim of TM perforation, with the epithelium then guided to migrate until the TM perforation is closed. Compared to the temporal fascia grafting technique, the paper-patch technique uses only the rim of the perforation with the remaining area of TM untouched. However, after healing of the perforation, there is still a ABG present. For example, Park et al.¹⁹ reviewed 27 cases of TM perforation without middle ear pathology. Their results showed that even for cases with a perforation of less than 5% of the total TM area, there was still a ABG present after paper-patch healing. The main reason argument being that the fiber layer of the TM at the perforation area could not be regenerated to normal,³⁴ and that fiber layer plays a key role for the middle ear transfer function especial a high frequencies.³⁷

As mentioned above, the size, density, and Young's modulus of the repaired TM affects the TM's vibration. Unfortunately, only pure tone audiometry, middle ear analyzer, and computerized tomography (CT) can be used by ear surgeons to analyze the vibration of a repaired TM. The middle ear analyzer, measuring the impedance or admittance of the middle ear, has no direct information between the ABG and repaired TM. And the clinical CT with thickness resolution of .5–.625 mm, neither delineates the material properties of the reconstructed TM nor the detailed cues between ABG and TM perforation. In addition, the material properties of a repaired TM are also unavailable in vivo post-myringoplasty.

Displacement of the TM at 80 dB SPL is less than 100 nm,¹¹ the resolution of the surgical microscope is more than 1 μ m. This means that what can be seen of the movement of the TM using a surgical microscope is unphysiological. Therefore, cases with a normal tympanogram and CT scan but having a residual ABG cannot be explained using clinical data.

Our previous published data²⁵ showed that the repaired TM vibration post-myringoplasty is correlated with ABG after an operation, especially at 1 kHz. In that study, the LDV method was used to measure the vibration of the repaired TM in the

patient. The LDV method for live humans⁴¹⁻⁴⁶ could provide additional TM vibration and ABG information.

Caveats

There is a methodological caveat within this study. Air-bone gap is the pure tone threshold difference between air and BC in audiometry and is an important indicator of middle ear transfer function.²⁵ We only measured vibration of the TM at the umbo as the indicator of ABG rather than the difference between vibrations of the TM and the stapes footplate.²⁷ In addition, as shown in Figure 3, there is a discrepancy in the normative TM displacement at the umbo of the FE model when compared to the TB model. This is mainly due to the FE model used in this study. This model does not include the external auditory canal, and thereby the calculated middle ear transfer function would be affected at the resonance frequency.^{11,47} As the material properties of a repaired TM after myringoplasty are variable, the material properties of the FE model cannot be exactly the same as the material properties of the paper patch.

Conclusions

The results of this study show that as the size of perforation increases there is a concomitant decrease in the vibration of the TM at the umbo. After perforation repair, an ABG was still observed in TB and the FE models. Furthermore, when the TM perforation was enlarged to 50% of the total TM area, the cone shape of the TM disappeared and the density and stiffness of the TM changed, the vibration of TM at the umbo could be reduced by approximately 30 dB at 1000 Hz, and approximately 20 dB at the other frequencies. The material properties and anatomical shape of the repaired TM could affect vibration of the repaired TM, which could influence the modal motion and the wave motion of the TM. This effect could not be observed using the current clinical instruments.

Declaration of Conflicting Interests

The author(s) declared no potential conflicts of interest with respect to the research, authorship, and/or publication of this article.

Funding

The author(s) disclosed receipt of the following financial support for the research, authorship, and/or publication of this article: This research was funded by Great Britain Sasakawa Foundation (5826), Cardiff Metropolitan University Research Innovation Award and The Global Academies Research and Innovation Development Fund. Professor Fei Zhao won Global Academies and Santandar 2021 Fellowship Award.

ORCID iDs

Xingmei Wei  <https://orcid.org/0000-0001-7188-485X>

References

1. Morris P. Chronic suppurative otitis media. *BMJ Clin Evid*. 2012;2012:0507.
2. Dawood MR. Hearing evaluation after successful myringoplasty. *J Otolaryngol*. 2017;12(4):192-197. doi:10.1016/j.joto.2017.08.005
3. Storrs L. Myringoplasty. *Laryngoscope*. 1966;76(2):185-195. doi:10.1288/00005537-196602000-00001
4. Phillips JS, Yung MW, Nunney I. Myringoplasty outcomes in the UK. *J Laryngol Otol*. 2015;129(9):860-864. doi:10.1017/S002221511500198X
5. Pfammatter A, Novoa E, Linder T. Can myringoplasty close the air-bone gap? *Otol Neurotol*. 2013;34(4):705-710. doi:10.1097/MAO.0b013e3182898550
6. Nardone M, Sommerville R, Bowman J, Danesi G. Myringoplasty in simple chronic otitis media: Critical analysis of long-term results in a 1,000-adult patient series. *Otol Neurotol*. 2012;33(1):48-53. doi:10.1097/MAO.0b013e31823dbc26
7. Shrestha S, Sinha BK. Hearing results after myringoplasty. *Kathmandu Univ Med J*. 2006;4(4):455-459.
8. Thiel G, Mills RP, Mills N. Factors affecting hearing improvement following successful repair of the tympanic membrane. *J Laryngol Otol*. 2013;127(4):349-353. doi:10.1017/S0022215113000157
9. Rosowski JJ, Cheng JT, Merchant SN, Harrington E, Furlong C. New data on the motion of the normal and reconstructed tympanic membrane. *Otol Neurotol*. 2011;32(9):1559-1567. doi:10.1097/MAO.0b013e31822e94f3
10. Gan RZ, Cheng T, Dai CK, Yang F, Wood MW. Finite element modeling of sound transmission with perforations of tympanic membrane. *J Acoust Soc Am*. 2009;126(1):243-253. doi:10.1121/1.3129129
11. Koike T, Wada H, Kobayashi T. Modeling of the human middle ear using the finite-element method. *J Acoust Soc Am*. 2002;111(3):1306-1317. doi:10.1121/1.1451073
12. Luers JC, Huttenbrink KB. Surgical anatomy and pathology of the middle ear. *J Anat*. 2016;228(2):338-353. doi:10.1111/joa.12389
13. Roosli C, Chhan D, Halpin C, Rosowski JJ. Comparison of umbo velocity in air- and bone-conduction. *Hear Res*. 2012;290(1-2):83-90. doi:10.1016/j.heares.2012.04.011
14. Lee CF, Chen JH, Chou YF, Hsu LP, Chen PR, Liu TC. Optimal graft thickness for different sizes of tympanic membrane perforation in cartilage myringoplasty: A finite element analysis. *Laryngoscope*. 2007;117(4):725-730. doi:10.1097/mlg.0b013e318031f0e7
15. Merchant SN, McKenna MJ, Rosowski JJ. Current status and future challenges of tympanoplasty. *Eur Arch Oto-Rhino-Laryngol*. 1998;255(5):221-228. doi:10.1007/s004050050047
16. Eldaibes M, Landry TG, Bance ML. Repair of subtotal tympanic membrane perforations: A temporal bone study of several tympanoplasty materials. *PLoS One*. 2019;14(9):e0222728. doi:10.1371/journal.pone.0222728
17. Voss SE, Rosowski JJ, Merchant SN, Peake WT. How do tympanic-membrane perforations affect human middle-ear sound transmission? *Acta Otolaryngol*. 2001;121(2):169-173.
18. Roosli C, Sim JH, Chatzimichalis M, Huber AM. How does closure of tympanic membrane perforations affect hearing and

- middle ear mechanics?-An evaluation in a patient cohort and temporal bone models. *Otol Neurotol*. 2012;33(3):371-378. doi:[10.1097/MAO.0b013e31824296ee](https://doi.org/10.1097/MAO.0b013e31824296ee)
19. Park SN, Kim HM, Jin KS, Maeng JH, Yeo SW, Park SY. Predictors for outcome of paper patch myringoplasty in patients with chronic tympanic membrane perforations. *Eur Arch Oto-Rhino-Laryngol*. 2015;272(2):297-301. doi:[10.1007/s00405-013-2860-y](https://doi.org/10.1007/s00405-013-2860-y)
 20. Lee SH, Jin SM, Lee KC, Kim MG. Paper-patch myringoplasty with CO2 laser for chronic TM perforation. *Eur Arch Oto-Rhino-Laryngol*. 2008;265(10):1161-1164. doi:[10.1007/s00405-008-0592-1](https://doi.org/10.1007/s00405-008-0592-1)
 21. Golz A, Goldenberg D, Netzer A, et al. Paper patching for chronic tympanic membrane perforations. *Otolaryngol Head Neck Surg*. 2003;128(4):565-570. doi:[10.1016/s0194-5998\(03\)00124-4](https://doi.org/10.1016/s0194-5998(03)00124-4)
 22. Koike T, Wada H, Kobayashi T. Effect of depth of conical-shaped tympanic membrane on middle-ear sound transmission. *JSME Int J Series C Mech Syst, Machine Elements Manufac*. 2001;44(4):1097-1102. doi:[10.1299/jsmec.44.1097](https://doi.org/10.1299/jsmec.44.1097)
 23. Guthold M, Liu W, Sparks EA, et al. A comparison of the mechanical and structural properties of fibrin fibers with other protein fibers. *Cell Biochem Biophys*. 2007;49(3):165-181. doi:[10.1007/s12013-007-9001-4](https://doi.org/10.1007/s12013-007-9001-4)
 24. Luo H, Wang F, Cheng C, Nakmali DU, Gan RZ, Lu H. Mapping the Young's modulus distribution of the human tympanic membrane by microindentation. *Hear Res*. 2019;378:75-91. doi:[10.1016/j.heares.2019.02.009](https://doi.org/10.1016/j.heares.2019.02.009)
 25. Zhang Y, Wang J, Wang Y, Fu Q, Li Y. Association between the air-bone gap and vibration of the tympanic membrane after myringoplasty. *Ear Nose Throat J*. 2021;100(4):241-248. doi:[10.1177/0145561320983649](https://doi.org/10.1177/0145561320983649)
 26. Voss SE, Rosowski JJ, Merchant SN, Peake WT. Middle-ear function with tympanic-membrane perforations. I. Measurements and mechanisms. *J Acoust Soc Am*. 2001;110(3 Pt 1):1432-1444. doi:[10.1121/1.1394195](https://doi.org/10.1121/1.1394195)
 27. Voss SE, Rosowski JJ, Merchant SN, Peake WT. Middle-ear function with tympanic-membrane perforations. II. A simple model. *J Acoust Soc Am*. 2001;110(3 Pt 1):1445-1452. doi:[10.1121/1.1394196](https://doi.org/10.1121/1.1394196)
 28. Mehta RP, Rosowski JJ, Voss SE, O'Neil E, Merchant SN. Determinants of hearing loss in perforations of the tympanic membrane. *Otol Neurotol*. 2006;27(2):136-143. doi:[10.1097/01.mao.0000176177.17636.53](https://doi.org/10.1097/01.mao.0000176177.17636.53)
 29. Anthony WP, Harrison CW. Tympanic membrane perforation. Effect on audiogram. *Arch Otolaryngol*. 1972;95(6):506-510. doi:[10.1001/archotol.1972.00770080796003](https://doi.org/10.1001/archotol.1972.00770080796003)
 30. Voss SE, Rosowski JJ, Merchant SN, Peake WT. Non-ossicular signal transmission in human middle ears: Experimental assessment of the "acoustic route" with perforated tympanic membranes. *J Acoust Soc Am*. 2007;122(4):2135-2153. doi:[10.1121/1.2769617](https://doi.org/10.1121/1.2769617)
 31. Trojanowska A, Drop A, Trojanowski P, Rosinska-Bogusiewicz K, Klatka J, Bobek-Billewicz B. External and middle ear diseases: Radiological diagnosis based on clinical signs and symptoms. *Insights Imag*. 2012;3(1):33-48. doi:[10.1007/s13244-011-0126-z](https://doi.org/10.1007/s13244-011-0126-z)
 32. Urstöger G, Kulachenko A, Schennach R, Hirn U. Micro-structure and mechanical properties of free and restrained dried paper: A comprehensive investigation. *Cellulose*. 2020;27(15):8567-8583. doi:[10.1007/s10570-020-03367-4](https://doi.org/10.1007/s10570-020-03367-4)
 33. Stenfeldt K, Johansson C, Hellstrom S. The collagen structure of the tympanic membrane: collagen types I, II, and III in the healthy tympanic membrane, during healing of a perforation, and during infection. *Arch Otolaryngol Head Neck Surg*. 2006;132(3):293-298. doi:[10.1001/archotol.132.3.293](https://doi.org/10.1001/archotol.132.3.293)
 34. Gladstone HB, Jackler RK, Varav K. Tympanic membrane wound healing. An overview. *Otolaryngol Clin*. 1995;28(5):913-932.
 - Singh G, Chanda A. Mechanical properties of whole-body soft human tissues: a review. *Biomed Mater* 2021;16(6):1-25. doi:[10.1088/1748-605X/ac2b7a](https://doi.org/10.1088/1748-605X/ac2b7a).
 36. De Greef D, Pires F, Dirckx JJ. Effects of model definitions and parameter values in finite element modeling of human middle ear mechanics. *Hear Res*. 2017;344:195-206. doi:[10.1016/j.heares.2016.11.011](https://doi.org/10.1016/j.heares.2016.11.011)
 37. O'Connor KN, Tam M, Blevins NH, Puria S. Tympanic membrane collagen fibers: A key to high-frequency sound conduction. *Laryngoscope*. 2008;118(3):483-490. doi:[10.1097/MLG.0b013e31815b0d9f](https://doi.org/10.1097/MLG.0b013e31815b0d9f)
 38. Parent P, Allen JB. Wave model of the cat tympanic membrane. *J Acoust Soc Am*. 2007;122(2):918-931. doi:[10.1121/1.2747156](https://doi.org/10.1121/1.2747156)
 39. Cheng JT, Hamade M, Merchant SN, Rosowski JJ, Harrington E, Furlong C. Wave motion on the surface of the human tympanic membrane: Holographic measurement and modeling analysis. *J Acoust Soc Am*. 2013;133(2):918-937. doi:[10.1121/1.4773263](https://doi.org/10.1121/1.4773263)
 40. Parent P, Allen JB. Time-domain "wave" model of the human tympanic membrane. *Hear Res*. 2010;263(1-2):152-167. doi:[10.1016/j.heares.2009.12.015](https://doi.org/10.1016/j.heares.2009.12.015)
 41. Archvo I, Lasurashvili N, Bornitz M, Kevanishvili Z, Zahnert T. Laser Doppler vibrometry of the middle ear in humans: derivation dependence, variability, and bilateral differences. *Medicina-Lithuania*. 2009;45(11):878-886. doi:[DOI 10.3390/medicina45110113](https://doi.org/10.3390/medicina45110113)
 42. Goode RL, Ball G, Nishihara S, Nakamura K. Laser Doppler vibrometer (LDV) - A new clinical tool for the otologist. *Am J Otol*. 1996;17(6):813-822.
 43. Huber AM, Schwab C, Linder T, et al. Evaluation of eardrum laser Doppler interferometry as a diagnostic tool. *Laryngoscope* 2001; 111(3):501-507. doi:[10.1097/00005537-200103000-00022](https://doi.org/10.1097/00005537-200103000-00022)
 44. Jakob A, Bornitz M, Kuhlisch E, Zahnert T. New aspects in the clinical diagnosis of otosclerosis using laser doppler vibrometry. *Otol Neurotol*. 2009;30(8):1049-1057. doi:[10.1097/MAO.0b013e31819e622b](https://doi.org/10.1097/MAO.0b013e31819e622b)
 45. Jie Wang FZ, Zhang Y, Li Y. Measurement of tympanic membrane motion in normal adults using laser doppler vibrometry. *Chin J Otol*. 2016;14(3):330-333. doi:[10.3969/j.issn.1672-2922.2016.03.003](https://doi.org/10.3969/j.issn.1672-2922.2016.03.003)
 46. Whittemore KR, Merchant SN, Poon BB, Rosowski JJ. A normative study of tympanic membrane motion in humans using a laser Doppler vibrometer (LDV). *Hearing Res*. 2004;187(1-2):85-104. doi:[10.1016/S0378-5955\(03\)00332-0](https://doi.org/10.1016/S0378-5955(03)00332-0)
 47. Gan RZ, Sun Q, Dyer RK Jr., Chang KH, Dormer KJ. Three-dimensional modeling of middle ear biomechanics and its applications. *Otol Neurotol*. 2002;23(3):271-280. doi:[10.1097/00129492-200205000-00008](https://doi.org/10.1097/00129492-200205000-00008)